LETTERS

Tracking the motion of charges in a terahertz light field by femtosecond X-ray diffraction

A. Cavalleri[1,2], S. Wall[1], C. Simpson[1], E. Statz[3], D. W. Ward[3], K. A. Nelson[3], M. Rini[4] & R. W. Schoenlein[4]

In condensed matter, light propagation near resonances is described in terms of polaritons, electro-mechanical excitations in which the time-dependent electric field is coupled to the oscillation of charged masses[1,2]. This description underpins our understanding of the macroscopic optical properties of solids, liquids and plasmas, as well as of their dispersion with frequency. In ferroelectric materials, terahertz radiation propagates by driving infrared-active lattice vibrations, resulting in phonon-polariton waves. Electro-optic sampling with femtosecond optical pulses[3–5] can measure the time-dependent electrical polarization, providing a phase-sensitive analogue to optical Raman scattering[6,7]. Here we use femtosecond time-resolved X-ray diffraction[8–10], a phase-sensitive analogue to inelastic X-ray scattering[11–13], to measure the corresponding displacements of ions in ferroelectric lithium tantalate, $LiTaO_3$. Amplitude and phase of all degrees of freedom in a light field are thus directly measured in the time domain. Notably, extension of other X-ray techniques to the femtosecond timescale (for example, magnetic or anomalous scattering) would allow for studies in complex systems, where electric fields couple to multiple degrees of freedom[14].

Below $T_c \approx 900\,^{\circ}C$, $LiTaO_3$ is ferroelectric, with a permanent *c*-axis structural distortion coupled to a permanent electric dipole. At terahertz frequencies, light couples with periodic lattice distortions around the ferrolectric equilibrium positions, resulting in a phonon-polariton mode of A_1 symmetry. Because of the reduced symmetry of the ferroelectric phase, $LiTaO_3$ has also a large optical nonlinearity, and consequently femtosecond visible pulses can be used to generate terahertz radiation by means of impulsive stimulated Raman scattering (ISRS). The resulting time-dependent electrical polarization of coherent phonon polaritons has been measured in a number of experiments with electro-optic sampling, spatiotemporal imaging and other optical observables at visible frequencies. However, the corresponding lattice motions have to date remained undetected, leading sometimes to controversy on the interpretation of coherent polariton experiments[15]. Here we use femtosecond X-rays to measure the corresponding atomic oscillations[16], which we compare with a time-domain simulation of terahertz propagation to extract the absolute displacements with 1-mÅ resolution.

Figure 1a shows a sketch of the experimental geometry. Coherent phonon polaritons in $LiTaO_3$ were excited nonlinearly at the surface by a 70-fs, *s*-polarized, 800-nm laser pulse at a fluence of 10 mJ cm^{-2}. Terahertz lattice distortions were then measured directly as time-dependent modulations of the 006 structure factor. To maximize the temporal resolution of our experiments, the 68° incidence angle for both pump and probe (22° according to the X-ray convention) was then dictated by the Bragg condition for the 7-keV X-ray probe. A finite-difference time-domain simulation, describing the excitation and propagation of phonon-polaritons[17] at arbitrary angles, was used

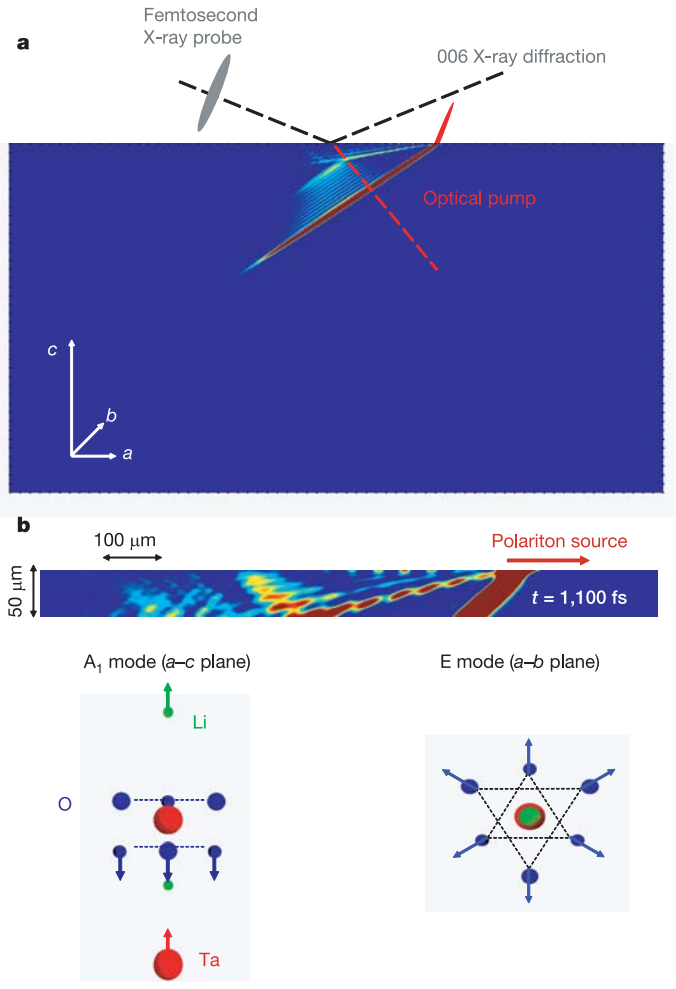

Figure 1 | Excitation of phonon polaritons in $LiTaO_3$. **a**, Experimental geometry. Phonon-polaritons were excited via ISRS with *s*-polarized, 70-fs pulses of near-800-nm wavelength at a fluence of 10 mJ cm^{-2}. The optical pump pulse impinged onto the sample at the 68° angle, as dictated by the Bragg condition for the 7-keV, X-ray diffraction probe. The pump pulse was thus refracted at a 32° angle and generated a time- and space-dependent pattern of terahertz phonon-polaritons. The lattice distortions along the *c* axis of $LiTaO_3$ were measured as modulations of the 006 structure factor. **b**, Snapshot of the spatial pattern of polaritons. The figure shows a 40-μm-wavelength surface wave with propagation along the surface normal. The measured lattice distortions associated with the A_1 and E modes are shown. The polarization component in the *a*–*b* plane, associated with a vibrational mode of E symmetry, is not detected in this reflection.

[1]Department of Physics, Clarendon Laboratory, University of Oxford, Oxford OX1 3PU, UK. [2]Central Laser Facility & Diamond Light Source, Rutherford Appleton Laboratory, Chilton, Didcot, OX11 0QX, UK. [3]Department of Chemistry, Massachusetts Institute of Technology, Cambridge, Massachusetts 02139, USA. [4]Materials Sciences Division, Lawrence Berkeley National Laboratory, Berkeley, California 94720, USA.

to predict and interpret the experimental results. In our simulations, the terahertz radiation field was coupled linearly to the lattice vibrations, which were treated as a driven ionic oscillator. The relevant lattice vibrations and their coupling to electromagnetic radiation were described through an auxiliary parameter, which accounted for the potential-energy surface of the specific phonon-mode. Lattice vibrations contributed to the terahertz radiation field through the ionic polarization, which was linear in the ionic displacement. Polariton generation with femtosecond optical pulses of arbitrary time duration and fluence was described by an additional driving term to the ionic oscillator that is proportional to the ISRS excitation intensity.

A snapshot of the simulated phonon-polariton pattern, calculated at first with a coarse 5-μm spatial mesh, is also displayed in Fig. 1a. The 800-nm pump pulse was refracted at 32° from the surface normal and two polariton waves propagated at a slower group velocity in the wake of the laser pulse. The first terahertz wave followed at the same 32° angle of the optical pump, while a second one propagated at 8° from the surface normal.

A higher-resolution simulation, reported in Fig. 1b, explains the excitation mechanism. Refraction of the 800-nm pump pulse over the 1-mm^2 spot resulted in an optical wave front that crossed the vacuum–material interface at different points for different time delays. The 21-μm length of the 70-fs optical pulse corresponded then to a nonlinear 'source' that travelled along the surface at an effective speed of $1.08c_0$, where c_0 is the speed of light in vacuum. This speed is only apparent, and does not imply superluminal propagation.

In the spirit of the Huygen's principle, and keeping into account both linear (800-nm) and nonlinear (terahertz) terms, the re-radiated field can be broken into three components: (1) The linearly re-radiated optical field propagates into the solid at $c_0/2.25$, where $n \approx 2.25$ is the index of refraction of $LiTaO_3$ at 800 nm. This effect results in conventional refraction at 32° from the surface normal. (2) The terahertz waves generated beneath the surface followed the optical pump–pulse at the same 32° angle. (3) A second wave at terahertz frequencies was also generated at the very surface, resulting from a moving nonlinear source that was matched to a wave propagating into the solid at a speed of $c_0/6.1$ ($n \approx 6.1$), resulting in propagation at 8° from the surface normal. The 40-μm wavelength for the terahertz radiation was then dictated by the projection onto the *a*–*b* plane of the longitudinal width of the optical pulse (~21 μm/cosine68°). Thus, a 1.5-THz wave entered the solid as if it were impinging from vacuum collinearly with the optical pulse and as if it were refracted linearly into the material.

Two polarization components were excited in the terahertz field, one parallel and one perpendicular to the optic axis of $LiTaO_3$. These were associated with two different vibrational modes of the crystal, one of A_1 symmetry along the *c* (or optic) axis, and one of E symmetry in the *a*–*b* plane. Figure 1b shows the atomic displacements for these two normal modes. Diffraction from the 006 plane was insensitive to all distortions of the unit cell in the *a*–*b* plane, which can only be detected for nonzero *h* and/or *k* (two of the three Miller indices, for an *hkl* X-ray reflection). Thus, our experiment could only detect distortions of A_1 symmetry along the *c* axis.

Optical pump, X-ray probe experiments were performed by using synchrotron radiation from laser-modulated electron bunches[18–20], which interacted with the optical field within a wiggler of the storage ring (see Fig. 2). Two energy sidebands at approximately 10 MeV from the 1.9-GeV central energy of the beam were impressed by interaction of the electron beam with the optical field. Femtosecond electron bunches were then transiently separated from the main orbit in the next bending magnet, where the electron beam energy was dispersed along the radius of the storage ring. Femtosecond synchrotron radiation was thus imaged onto the sample using a toroidally bent silicon mirror, and resulted in X-ray pulses that were separated by approximately 500 μm from the main axis of the beam. Broadband, femtosecond X-rays were passed through a two-crystal Si-111 monochromator, producing a train of monochromatic X-ray pulses at 7 keV. The spot size of the probing X-rays was of approximately 200 μm × 150 μm, projected over a surface region approximately 300-μm long, due to the 68° angle of incidence (measured from the surface normal). The detected flux in the femtosecond X-rays was approximately four orders of magnitude lower than in the picosecond pulse, amounting to a few thousand photons per second of 0.1% bandwidth in a 2-kHz train. After diffraction, a few hundred photons per second were detected by the avalanche photo diode (APD). A cross-correlation between the pump laser and the sliced

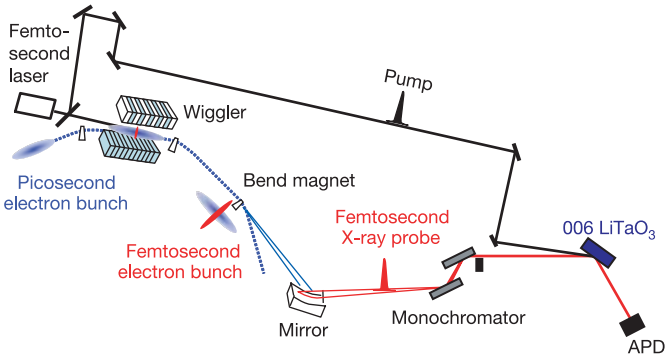

Figure 2 | Optical pump, X-ray diffraction probe experimental apparatus. A single Ti:Sa laser oscillator was synchronized to the storage-ring orbit clock to about 1 ps. These low-energy pulses were amplified in two separate regenerative amplifiers. The laser pulses used to impress energy modulation onto the electron bunches and those used to excite the sample were derived from the same oscillator, ensuring absolute synchronization between optical pump and X-ray probe. Time-dependent modulations of the integrated 006 diffraction peak were measured at 7 keV as a function of the pump–probe time delay.

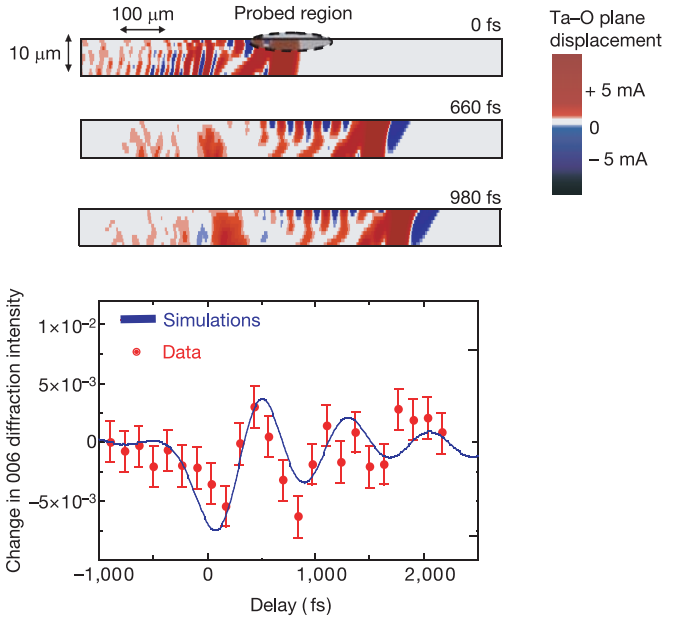

Figure 3 | Measurement of the time-dependent change in the 006 diffracted intensity. The error bars in the time-dependent X-ray diffraction data represent one standard deviation of the shot-noise-limited distribution of detected photons. In the three simulated patterns, the colour code represents the absolute displacement of the Ta atom with respect to the plane of oxygen atoms, taking positive and negative values with respect to the equilibrium (distorted) positions. The continuous curve in the lower panel is then a one-parameter fit to the measured experimental data.

pulses of visible bending magnet radiation revealed a pulse duration of approximately 200 fs.

Figure 3 displays the measured time-dependent scattering intensity. A 1.5-THz modulation of the 006 structure factor was found, with a sine-like time dependence that reflects the electronic-ground-state nature of lattice motions initiated with ISRS. The data were compared to the results of the polariton propagation simulation, which were performed with submicrometre resolution and are also shown in Fig. 3. The colour code of the polariton pattern represents the amplitude of the *c*-axis displacements of the A_1 mode, highlighting positive and negative motion of the Ta with respect to the oxygen plane. The sub-surface polariton patterns were combined with the time- and space-dependent displacements of the A_1 normal mode of Fig. 1b, and were integrated spatially over the probed volume to account for the change in the 006 X-ray reflectivity. The continuous curve superimposed on the data displays the results of our simulation. Importantly, because the extinction depth was of less than 1 μm, our femtosecond X-ray diffraction experiments sampled only the polariton wave immediately beneath the surface. Because the probed near-surface volume was homogeneously excited at all times, dynamic diffraction simulations gave identical results to those obtained in the kinematic approximation.

No free parameter was left in the calculation, except for the absolute displacements of the A_1 normal mode, which were adjusted to fit the data. The colour code of Fig. 3 shows a 5-mA peak motion of the Ta atom with respect to the plane of the oxygen atoms. This motion corresponds to approximately 3% of what is needed to reach the ferroelectric phase at higher temperatures ($T_c = 900$ K).

In summary, we used femtosecond X-ray diffraction to measure the lattice motions that sustain terahertz light propagation in ferroelectric $LiTaO_3$. Ultrafast lattice motions along the A_1 lattice direction were driven by phonon-polaritons excited at the solid–vacuum interface by ISRS. Our experiments and simulations reveal a polariton wave with a frequency of 1.5 THz, as set by the pulse duration and angle of incidence of our optical pulse. Similar experiments with improved X-ray focusing capabilities would allow for the imaging of space- and time-dependence in this and similar problems, allowing for full mapping of coherently excited lattice waves[21]. Femtosecond X-ray measurements could also be coupled to high-amplitude lattice excitation, to drive the structure into transient or permanent states that are not accessed near equilibrium.

More generally, ultrafast X-ray diffraction from terahertz lattice waves opens the way to new dynamic studies in complex solids in their electronic ground state, in which microscopic couplings among multiple degrees of freedom dominate the physics[22–24]. Finally, the possibility of controlling propagating phonon-polariton modes may result in new concepts for ultrafast Bragg switches[25,26], capable of separating femtosecond slices from longer X-ray pulses.

Received 1 May; accepted 30 June 2006.

1. Mills, D. L. & Burstein, E. Polaritons: the electromagnetic modes of media. *Rep. Prog. Phys.* **37,** 817–926 (1974).
2. Barker, A. S. Jr & Loudon, R. Response functions in the theory of Raman scattering by vibrational and polariton modes in dielectric crystals. *Rev. Mod. Phys.* **44,** 18–47 (1972).
3. Auston, D. H., Cheung, K. P., Valdamanis, J. A. & Kleinman, D. Cherenkov radiation from femtosecond optical pulses in electro-optic media. *Phys. Rev. Lett.* **53,** 1555–1558 (1984).
4. Wahlstrand, J. K. & Merlin, R. Cherenkov radiation emitted by ultrafast laser pulses and the generation of coherent polaritons. *Phys. Rev. B* **68,** 054301 (2003).
5. Crimmins, T. F., Stoyanov, N. S. & Nelson, K. A. Heterodyned impulsive stimulated Raman scattering of phonon-polaritons in $LiTaO_3$ and $LiNbO_3$. *J. Chem. Phys.* **117,** 2882–2896 (2002).
6. Dougherty, T. P. *et al.* Femtosecond resolution of soft mode dynamics in structural phase transitions. *Science* **258,** 770–774 (1992).
7. Stevens, T. E., Wahlstrand, J. K., Kuhl, J. & Merlin, R. Cherenkov radiation at speeds below the light threshold: phonon assisted phase matching. *Science* **291,** 627–630 (2001).
8. Rischel, C. *et al.* Femtosecond time-resolved X-ray diffraction from laser heated organic films. *Nature* **390,** 490–492 (1997).
9. Cavalleri, A. *et al.* Femtosecond structural dynamics in VO_2 during an ultrafast solid-solid phase transition. *Phys. Rev. Lett.* **87,** 237401 (2001).
10. Lindenberg, A. M. *et al.* Atomic scale visualization of inertial dynamics. *Science* **308,** 392–395 (2005).
11. Cavalleri, A. *et al.* Anharmonic lattice dynamics in germanium measured with ultrafast x-ray diffraction. *Phys. Rev. Lett.* **85,** 586–589 (2000).
12. Lindenberg, A. M. *et al.* Time-resolved X-ray diffraction from coherent phonons during a laser-induced phase transition. *Phys. Rev. Lett.* **84,** 111–114 (2000).
13. Bargheer, M. *et al.* Coherent atomic motions in a nanostructure studied by femtosecond x-ray diffraction. *Science* **306,** 1771–1773 (2004).
14. Kimel, A. V. *et al.* Ultrafast non-thermal control of magnetization by instantaneous photo-magnetic pulses. *Nature* **435,** 655–657 (2005).
15. Bakker, H. J., Hunsche, S. & Kurz, H. Time-resolved study of phonon polaritons in $LiTaO_3$. *Phys. Rev. B* **48,** 13524–13537 (1993).
16. Sokolowski-Tinten, K. *et al.* Femtosecond X-ray measurement of coherent lattice vibrations near the Lindemann stability limit. *Nature* **422,** 287–289 (2003).
17. Stoyanov, N. S., Ward, D. W., Feurer, Th. & Nelson, K. A. Terahertz polariton propagation in patterned materials. *Nature Mater.* **1,** 95–98 (2002).
18. Zholents, A. A. & Zolotorev, M. S. Femtosecond X-ray pulses of synchrotron radiation. *Phys. Rev. Lett.* **76,** 912–915 (1996).
19. Schoenlein, R. W. *et al.* Generation of femtosecond pulses of synchrotron radiation. *Science* **287,** 2237–2240 (2000).
20. Cavalleri, A. *et al.* Band selective measurements of electron dynamics in VO_2 using femtosecond near edge X-ray absorption. *Phys. Rev. Lett.* **95,** 067405 (2005).
21. Feurer, T., Vaughan, J. C. & Nelson, K. A. Spatiotemporal coherent control of lattice vibrational waves. *Science* **299,** 374–377 (2003).
22. Kimura, T. *et al.* Magnetic control of ferroelectric polarization. *Nature* **426,** 55–58 (2003).
23. Lottermoser, Th. *et al.* Magnetic phase control by an electric field. *Nature* **430,** 541–544 (2004).
24. Kimel, A. V., Kirilyuk, A., Tsvetkov, A., Pisarev, R. V. & Rasing, Th. Laser-induced ultrafast spin re-orientation in the antiferromagnet $TmFeO_3$. *Nature* **429,** 850–853 (2004).
25. Bucksbaum, P. H. & Merlin, R. The phonon Bragg switch: a proposal to generate sub-picosecond x-ray pulses. *Solid State Commun.* **111,** 535–539 (1999).
26. Nazarkin, A., Uschman, I., Förster, E. & Sauerbrey, R. High order Raman scattering of X-rays by optical phonons and generation of ultrafast X-ray transients. *Phys. Rev. Lett.* **93,** 207401 (2004).

Acknowledgements We thank M. Khalil for her help during data acquisition. We are grateful to J. S. Wark for discussions, as well as for sharing the results of dynamic diffraction simulations for $LiTaO_3$. We thank K. Sokolowski-Tinten, R. Merlin, D. Reis and S. Hooker for many discussions, suggestions and for critical reading of our manuscript. Help by N. Tamura with the measurement of static Laue patterns in $LiTaO_3$ is also gratefully acknowledged. Experiments at LBNL were supported by the Director, Office of Science, Office of Basic Energy Sciences, Division of Materials Science and Engineering Division, of the US Department of Energy. Work at the University of Oxford was supported by the European Science Foundation through a European Young Investigator Award. S.W. acknowledges receipt of a graduate scholarship from the UK Engineering and Physical Sciences Research Council. Simulation work at MIT was funded by the US National Science Foundation.

Author Information Reprints and permissions information is available at npg.nature.com/reprintsandpermissions. The authors declare no competing financial interests. Correspondence and requests for materials should be addressed to A.C. (a.cavalleri1@physics.ox.ac.uk).